A Quasi-Lagrangian Study of the Barotropic Jet Stream[1]

DAVID D. HOUGHTON
National Center for Atmospheric Research, Boulder, Colo.

(Manuscript received 19 April 1965, in revised form 8 July 1965)

ABSTRACT

A quasi-Lagrangian formulation for an inviscid barotropic fluid is presented and shown to afford a convenient basis for analysis of certain ageostrophic jet flows. Material lines serve as the references to delineate the north-south variations in the fluid, and Eulerian representation is used in the east-west direction. Several desirable features are shown for the use of material lines in this manner. First, by orienting the lines approximately parallel to the jet axis, flows with finite horizontal curvature may be represented simply. This is illustrated by a development with east-west variations represented by only two harmonics and a mean. The solution of this semi-spectral model agrees closely with a non-spectral numerical solution for over three days. Second, the Lagrangian movement of the material lines gives an indication of non-linear adjustment motions and demonstrates a mixing in the fluid.

1. Introduction

An understanding of jet streams is fundamental to the study of many synoptic-scale atmospheric phenomena. This is particularly evident in middle latitudes where jet streams are frequently associated with frontal zones and large-scale precipitation areas. A knowledge of the mechanisms of development and movement of the jet stream is, therefore, of rather general interest.

The characteristic large fluid velocity in a jet stream presents certain difficulties in theoretical analysis. Since in the general case it is necessary to consider motions with both a relatively large Rossby number and a significant ageostrophic component, the problem is clearly three-dimensional and non-linear. Much of the previous work on jet stream dynamics has dealt with the linearized problem, stability of zonal jet flows. The few theoretical studies concerned with the evolution of jets have used specialized models and have employed many simplifications. For example, Thompson (1957) found a time-dependent solution for the zonally averaged jet flow in a barotropic fluid by making certain assumptions concerning the statistics of the eddy motions.

The present study was made to investigate the utility of a quasi-Lagrangian representation for jet stream analysis. The fluid characteristics of the atmosphere suggest that a Lagrangian viewpoint is a natural basis for its study. However, the mathematical complexities of Lagrangian formulation are well known, and have prevented its use in the study of many problems. It was felt that a quasi-Lagrangian approach would avoid some of these mathematical complexities and yet provide a useful Lagrangian element to the analysis.

Quasi-Lagrangian constructions have been proposed and discussed in previous studies of atmospheric motions. Starr (1945) provided a systematic development of the method which had been employed and implied in earlier studies in meteorology and oceanography. Eliassen (1962) developed this concept further with special emphasis on the possibilities of its use with numerical prediction models. Most of the previous work has employed the Lagrangian coordinate for representation of the vertical direction.

In the present study a Lagrangian representation is used for one of the horizontal coordinates, namely the y or north-south coordinate. Such a quasi-Lagrangian system has been proposed previously for a horizontal coordinate. Freeman (1956) conducted some studies using such a system and specified that the material coordinate elements be lines of constant potential vorticity or absolute vorticity, whichever was the conservative quantity in the model under consideration. His purpose was to develop a set of approximate equations which could be analyzed by the method of characteristics.

The current investigation is made with a barotropic model for which the quasi-Lagrangian equations are easily formulated. Solutions are obtained for both the quasi-Lagrangian and Eulerian form of the equations. The former are solved by a spectral method and the latter by a straight-forward finite-difference approach. The Eulerian solution is made to provide a comparison to the solution of the quasi-Lagrangian equations. A straight-forward finite-difference solution could have been obtained for the quasi-Lagrangian equations, but it was felt that the spectral solution would demonstrate more of the potential of the quasi-Lagrangian system for analytic solutions.

[1] Presented at the AMS annual meeting, January 1965, New York, with the title "A Method for Analysis of Ageostrophic Barotropic Jet Streams."

2. Physical model

The model used in this study consists of an incompressible, barotropic, hydrostatic and inviscid fluid, existing in an infinite channel corresponding to a middle-latitude zonal band on the earth. The lower boundary is flat, the northern and southern boundaries are rigid walls, and the flow is periodic in the east-west direction. The tangent plane approximation is used which simplifies subsequent mathematical development and yet retains the geostrophic character of the flow.

In order to enhance the effects of horizontal divergence, the model is made to represent only the lower two-thirds of the atmosphere. This is achieved by placing a layer of infinite depth and lower density above the fluid of interest. Because of the differences in vertical scale, the pressure gradient in the lower fluid may be considered dependent only upon the slope of the interface between the fluids, with a value proportional to the difference in density between the layers. Therefore the model is equivalent to a barotropic fluid with a free upper boundary and a reduced acceleration of gravity. The reduction of gravity increases the Froude number and the effect of divergence in the flow. In order to approximate the stability of the U. S. Standard Atmosphere the effective acceleration of gravity is taken as 1.4 m sec^{-2} which means the density (corresponding to a potential density in the atmosphere) of the upper layer is 0.86 of that in the lower layer.

3. Quasi-Lagrangian coordinates

The basic feature of this study is the Lagrangian representation for the northward distance or y-dependency of the variables. The variable y is transformed from an independent variable in the Eulerian coordinates to a dependent variable which is a function of the remaining independent variables of the barotropic model, eastward distance and time (x and t), and the fluid "line" labeled by the identifier k. Thus $y=y(x,k,t)$ with k assumed to be a continuous variable. Any dependent variable, ϕ, for which a function exists in the Eulerian coordinates can be expressed in the quasi-Lagrangian system by the following transformation if $y(x,k,t)$ is a single-valued function in terms of x, k, and t:

$$\phi=A(x,y,t)=A[x,y(x,k,t),t]=B(x,k,t). \tag{1}$$

In order for derivatives of ϕ to exist, $y(x,k,t)$ must also be a continuously differentiable function. See Eliassen (1949) for further details of this transformation.

The elements of the Lagrangian coordinate are material lines in the horizontal plane whose movements are described by the function $y(x,k,t)$ satisfying the kinematic relationship,

$$\left.\frac{\partial y}{\partial t}\right|_k = v-u\left.\frac{\partial y}{\partial x}\right|_k, \tag{2}$$

where u is the east-west component of velocity and v the north-south component of velocity. Eq. (2) indicates that the dependent variable, v, is given explicitly by y and u. Thus the fundamental dependent variables in this quasi-Lagrangian barotropic model are fluid depth, x-component of velocity and northward distance (h, u and y, respectively). The requirement that $y(x,k,t)$ be both a single-valued and continuously differentiable function specifies that these material lines must never become oriented directly north-south, must never touch each other, and must extend continuously from one longitudinal lateral boundary to the other. The possibility of a north-south orientation in the material lines may be avoided by redefining them at suitable intervals of time or by considering flows which are sufficiently zonal.

One attribute of the quasi-Lagrangian coordinates is the discriminatory response to motions in the model. In the barotropic model two types of motion may be identified by linear analysis such as that done by Hinkelmann (1951). One type consists of "meteorological" waves (terminology of Phillips, 1960) and the other of gravity-inertial waves. Advection is fundamental to the former type. With the quasi-Lagrangian coordinates only gravity-inertial waves may be associated with motions moving entirely with respect to the material lines since these lines will respond to a large extent to the meteorological waves. Such discrimination assists in the analysis of adjustment mechanisms or the processes attempting to establish geostrophic equilibrium.

Another important attribute of the quasi-Lagrangian coordinate system is the simplification that may be possible in the representation of jet flows. By orienting the material lines parallel to the jet axis, variables may have a functional form where the north-south and east-west dependencies are rather well separated. Corresponding representation in Eulerian coordinates would require a functional form where no such separation is possible.

For example take the free-boundary height field given by

$$h(x,y)=\bar{H}+H\cos[\alpha(y-B\sin\lambda x)] \tag{3}$$

in Eulerian coordinates where $\bar{H}$ and H have units of depth, λ is the east-west wave number, α is the north-south wave number and B gives the amplitude in the y-direction of the sinusoidal pattern in the height ridges. In the quasi-Lagrangian coordinates this could be represented as

$$h(k)=\bar{H}+H\cos[\alpha kD] \tag{4}$$

if the northward distance of the material lines, y, is given by

$$y(x,k)=kD+B\sin\lambda x.$$

Here D is the north-south distance corresponding to a unit of k and is assumed to be a constant in this example.

4. Development of equations

The basic Eulerian equations for this model may be written:

$$\frac{\partial u}{\partial t}+u\frac{\partial u}{\partial x}+v\frac{\partial u}{\partial y}-fv+g\frac{\partial h}{\partial x}=0, \tag{5}$$

$$\frac{\partial v}{\partial t}+u\frac{\partial v}{\partial x}+v\frac{\partial v}{\partial y}+fu+g\frac{\partial h}{\partial y}=0, \tag{6}$$

$$\frac{\partial h}{\partial t}+u\frac{\partial h}{\partial x}+v\frac{\partial h}{\partial y}+h\left(\frac{\partial u}{\partial x}+\frac{\partial v}{\partial y}\right)=0, \tag{7}$$

where notation is as follows: x, east-west coordinate; y, north-south coordinate; t, time; u, velocity component in the x direction; v, velocity component in the y direction; h, depth; f, Coriolis parameter; and g, reduced acceleration of gravity. The y-component of velocity is zero at the northern and southern boundaries. Henceforth, the depth which is equivalent to the height of the free upper boundary will be referred to as the height.

Transformation of the equations to quasi-Lagrangian coordinates requires three differential relationships. Two are derived from the transformation (1) and apply to partial t and x derivatives,

$$\left.\frac{\partial\phi}{\partial t}\right|_{x,y}=\left.\frac{\partial\phi}{\partial t}\right|_{x,k}-\left.\frac{\partial\phi}{\partial y}\right|_{x,t}\left.\frac{\partial y}{\partial t}\right|_{x,k}, \tag{8}$$

$$\left.\frac{\partial\phi}{\partial x}\right|_{t,y}=\left.\frac{\partial\phi}{\partial x}\right|_{t,k}-\left.\frac{\partial\phi}{\partial y}\right|_{t,x}\left.\frac{\partial y}{\partial x}\right|_{t,k}. \tag{9}$$

The third puts y into the role of a dependent variable,

$$\left.\frac{\partial\phi}{\partial y}\right|_{x,t}=\left.\frac{\partial\phi}{\partial k}\right|_{x,t}\Big/\left.\frac{\partial y}{\partial k}\right|_{x,t}. \tag{10}$$

For simplicity the variable v is retained. This necessitates an additional equation, but it eliminates second order terms from the differential equations.

The quasi-Lagrangian equations may now be formulated by substituting Eqs. (8), (9) and (10) into (5), (6) and (7) then multiplying each by $\partial y/\partial k$ to eliminate fractions. The final equations are:

$$\frac{\partial y}{\partial k}\frac{\partial u}{\partial t}+\frac{\partial y}{\partial k}u\frac{\partial u}{\partial x}-\frac{\partial y}{\partial k}fv+\frac{\partial y}{\partial k}g\frac{\partial h}{\partial x}-g\frac{\partial h}{\partial k}\frac{\partial y}{\partial x}=0, \tag{11}$$

$$\frac{\partial y}{\partial k}\frac{\partial v}{\partial t}+\frac{\partial y}{\partial k}u\frac{\partial v}{\partial x}+\frac{\partial y}{\partial k}fu+g\frac{\partial h}{\partial k}=0, \tag{12}$$

$$\frac{\partial y}{\partial k}\frac{\partial h}{\partial t}+\frac{\partial y}{\partial k}u\frac{\partial h}{\partial x}+\frac{\partial y}{\partial k}h\frac{\partial u}{\partial x}-h\frac{\partial u}{\partial k}\frac{\partial y}{\partial x}+h\frac{\partial v}{\partial k}=0. \tag{13}$$

The set of equations is completed with Eq. (2),

$$\frac{\partial y}{\partial t}-v+u\frac{\partial y}{\partial x}=0. \tag{14}$$

Derivatives with respect to x and t are evaluated on the material lines. Note that north-south advection is evident only in the last equation which determines changes in the positions of the material lines.

5. Method of solution of the quasi-Lagrangian equations

As a demonstration of the suitability of the quasi-Lagrangian equations for analysis purposes, a spectral solution is obtained for the quasi-Lagrangian equations. A finite differencing with respect to the material lines is made in the north-south direction, and a spectral transformation is made in the east-west dependency of the variables. This method thus utilizes the periodic conditions that can be assumed in the direction of the flow but retains the portrayal of a realistic jet profile in the north-south direction.

The north-south finite differencing is done according to Lagrangian characteristics; namely the gradients are computed over a variable length corresponding to the north-south distance between chosen material lines. The following approximation is made for all derivatives with respect to k:

$$\frac{\partial\phi(x,k,t)}{\partial k}=\frac{\phi(x,k+\delta k,t)-\phi(x,k-k\delta,t)}{2\delta k}=\frac{\Delta\phi}{2\delta k},$$

where Δ indicates a centered finite difference, δk is the finite-difference interval in the k coordinate and ϕ is h, u, v or y. Eqs. (11) through (14) can then be written in the following forms:

$$\Delta y\frac{\partial u}{\partial t}+\Delta yu\frac{\partial u}{\partial x}-\Delta yfv+\Delta yg\frac{\partial h}{\partial x}-\Delta hg\frac{\partial y}{\partial x}=0, \tag{15}$$

$$\Delta y\frac{\partial v}{\partial t}+\Delta yu\frac{\partial v}{\partial x}+\Delta yfu+g\Delta h=0, \tag{16}$$

$$\Delta y\frac{\partial h}{\partial t}+\Delta yu\frac{\partial h}{\partial x}+\Delta yh\frac{\partial u}{\partial x}-h\Delta u\frac{\partial y}{\partial x}+h\Delta v=0, \tag{17}$$

$$\frac{\partial y}{\partial t}-v+u\frac{\partial y}{\partial x}=0. \tag{18}$$

It is observed that triply non-linear terms are present which will complicate any spectral transformation. The saving factor here is that very few harmonics are used.

The following substitutions are made:

$$\begin{bmatrix} u(x,k,t) \\ v(x,k,t) \\ h(x,k,t) \\ y(x,k,t) \end{bmatrix} = \begin{bmatrix} U_0(k,t) \\ V_0(k,t) \\ H_0(k,t) \\ Y_0(k,t) \end{bmatrix} + \sum_{j=1}^{N} \left\{ \begin{bmatrix} U_j(k,t) \\ V_j(k,t) \\ H_j(k,t) \\ Y_j(k,t) \end{bmatrix} \cos j\lambda x + \begin{bmatrix} u_j(k,t) \\ v_j(k,t) \\ h_j(k,t) \\ y_j(k,t) \end{bmatrix} \sin j\lambda x \right\}, \tag{19}$$

where j is the integer identifying each harmonic, N is the total number of harmonics, λ is the fundamental wave number in the x-direction and matrix notation is employed. By substituting these into the Eqs. (15) through (18), and equating coefficients of similar trigonometric functions, ordinary differential equations giving the time changes in the Fourier coefficients may be obtained. These are sets of simultaneous equations for the time-differentiated u, v, and h coefficients since the terms containing the time derivatives of these variables in the original equations are non-linear. The ordinary differential equations are of the form,

$$(P)\cdot \begin{bmatrix} \dot{U}_0(k,t) \\ \dot{U}_1(k,t) \\ \vdots \\ \dot{U}_N(k,t) \\ \dot{u}_1(k,t) \\ \vdots \\ \dot{u}_N(k,t) \end{bmatrix} = \begin{bmatrix} A_0(k,t) \\ A_1(k,t) \\ \vdots \\ A_N(k,t) \\ a_1(k,t) \\ \vdots \\ a_N(k,t) \end{bmatrix} \tag{20}$$

for the Fourier coefficients of u with a similar set of equations for the Fourier coefficients of v and h. The superdot denotes time differentiation and P is a square $2N+1$ by $2N+1$ matrix of linear elements, functions of the spectral components of y. The elements A_0, A_1, $\cdots$ A_N, a_1, $\cdots$ a_N are rather complicated expressions, functions of the Fourier coefficients. The equations for the coefficients of the displacement, y, are simpler as P is the unit matrix giving a set of independent equations for the time-differentiated coefficients.

These equations are solved with series of two harmonics ($N=2$) by a 4th order Adam-Moulton method of integration (Hildebrand, 1956). The integration has a time step which varies according to the time rate of change of the variables.

6. Method of solution of the Eulerian equations

A solution is obtained for the Eulerian equations by numerically integrating finite-difference equivalents. They are first written in momentum-flux form which can be symbolized as follows:

$$\frac{\partial E}{\partial t}+\frac{\partial F}{\partial x}+\frac{\partial G}{\partial y}+R=0 \tag{21}$$

where E, F, G and R are column matrices:

$$E=\begin{bmatrix} uh \\ vh \\ h \end{bmatrix}, \qquad F=\begin{bmatrix} u^2h+\frac{1}{2}gh^2 \\ uvh \\ uh \end{bmatrix},$$

$$G=\begin{bmatrix} uvh \\ v^2h+\frac{1}{2}gh^2 \\ vh \end{bmatrix}, \quad R=\begin{bmatrix} -fvh \\ fuh \\ 0 \end{bmatrix}.$$

These equations are put into a finite-difference form and integrated by the second-order two-step Lax-Wendroff scheme discussed by Richtmyer (1963). The grid is square with a space increment of Δx and a time step of Δt. The following finite-difference equations are used where the subscripts, l and m, and superscript, n, represent ordered positions in the x-direction, y-direction and time, respectively:

$$E_{l,m}{}^{n+1}=\tfrac{1}{4}(E^n{}_{l+1,m}+E^n{}_{l-1,m}+E^n{}_{l,m+1}+E^n{}_{l,m-1}) - \frac{\Delta t}{2\Delta x}(F^n{}_{l+1,m}-F^n{}_{l-1,m}+G^n{}_{l,m+1}-G^n{}_{l,m-1}) - \Delta t R^n{}_{l,m}, \tag{22}$$

$$E_{l,m}{}^{n+2}=E^n{}_{l,m}-\frac{\Delta t}{\Delta x}(F_{l+1,m}{}^{n+1}-F_{l-1,m}{}^{n+1} +G_{l,m+1}{}^{n+1}-G_{l,m-1}{}^{n+1})-2\Delta t R_{l,m}{}^{n+1}. \tag{23}$$

7. Calculations

Calculations were made using both of the methods just described with corresponding initial conditions and time and space increments for both cases. Henceforth, spectral or quasi-Lagrangian will refer to the first method presented and numerical or Eulerian will refer to the second method. The Eulerian calculations were done with a 79×96 point grid network with the 79 grids in the north-south direction. The grid spacing, Δx, was 60 km and the time step was four minutes. At no time was the von Neumann stability condition (without regard for Coriolis effects) violated. In order to make the quasi-Lagrangian calculations comparable with the numerical calculations, 79 material lines were used and except for near the northern and southern boundaries, the north-south distance between adjacent material lines was equal to 60 km everywhere initially. The error limits in the Adams-Moulton predictor-corrector scheme were set so that the integration would be performed with a time step of four minutes over most of the period of integration.

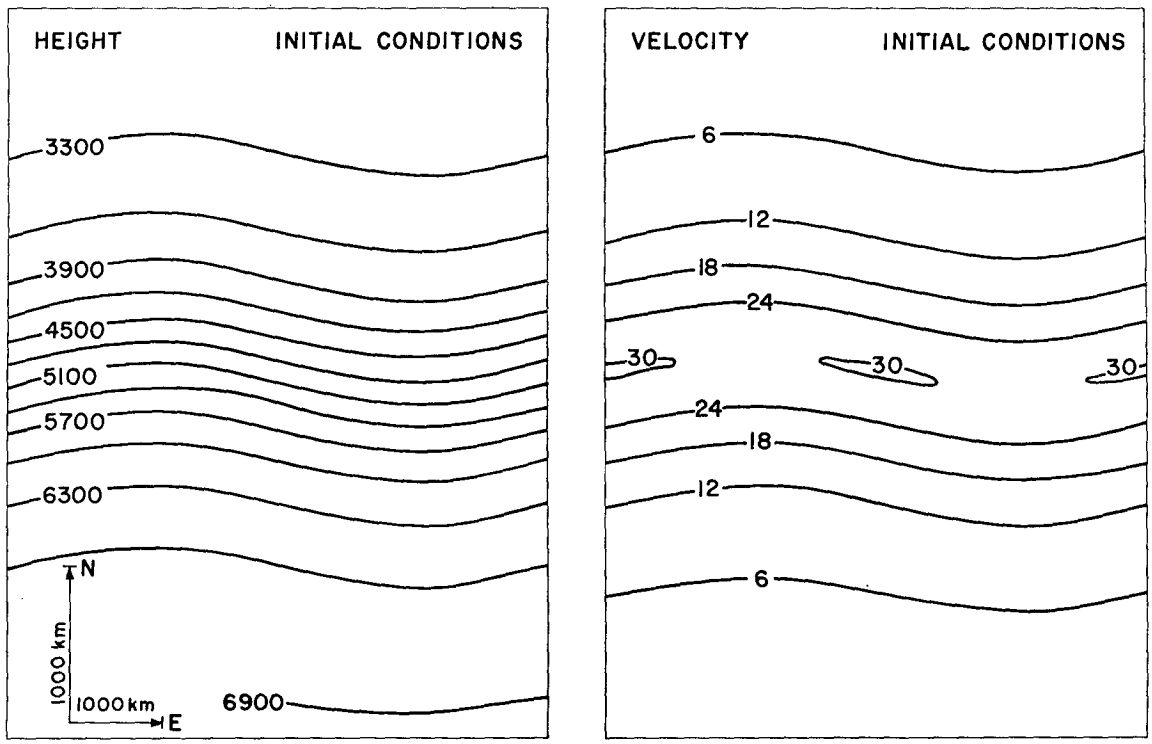

FIG. 1. Initial conditions for the calculations. Height (left side) is in meters and the velocity magnitude (right side) in meters per second. Distance scales are shown in the lower left hand corner.

The initial conditions were constructed such that representation in the quasi-Lagrangian coordinates would be simple. Initially the material lines were made to coincide with isotachs for the x-component of velocity and isopleths of height. Initial velocity was in geostrophic balance with the height field; isopleths of the latter had a horizontal sinusoidal oscillation of finite amplitude (see Fig. 1). Thus only the first harmonic was required, initially, to represent all the variables in the spectral model. This meant that the second harmonic had zero value, at first, assuring valid results for the truncated model for a finite period of time starting from $t=0$.

In the quasi-Lagrangian coordinates the rigid northern and southern boundaries had to be material lines. It was considered desirable to have a smooth transition from the space-oscillating material lines in the interior of the model to these fixed and straight lines. In order to simplify the mathematical treatment in the transition region, no attempt was made to match initial conditions between the spectral and numerical models near these boundaries. This discrepancy was not serious since most of the energy of the jet flow was concentrated well to the interior of the domain of integration.

The periodic boundary conditions for the eastern and western sides of the numerical grid matched exactly the periodicity in the spectral model; that is, the wave length of the first harmonic in the spectral model was set equal to the distance between the eastern and western boundaries of the numerical grid.

With l and m referring to ordered grid points in the eastward and northward directions, respectively, in the Eulerian model and k referring to ordered material lines in the quasi-Lagrangian model, the initial conditions for height, except near the northern and southern boundaries, were

$$h(l,m)=\bar{H}-H\tan^{-1}\left[\frac{m-m_0-B\sin\dfrac{2\pi l}{l_0}}{W}\right] \tag{24}$$

for the Eulerian model and

$$h(k)=\bar{H}-H\tan^{-1}\left[\frac{k-k_0}{W}\right] \tag{25}$$

in the quasi-Lagrangian model with the positions of the material lines given by

$$y(x,k)=Dk+B_0\sin\frac{2\pi x}{x_0} \tag{26}$$

everywhere except near the northern and southern boundaries. The following values were used: $\bar{H}=5000$ m, $H=1543$ m, $m_0=39$, $B=2$, $l_0=96$, $W=12$, $k_0=39$, $D=6\cdot10^4$m, $B_0=1.2\cdot10^5$m and $x_0=5.76\cdot10^6$m.

The x- and y-components of velocity were then ob-

tained from the geostrophic approximation as

$$u(l,m)=-\frac{g}{f}\left[\frac{h(l,m+1)-h(l,m-1)}{2\Delta x}\right], \quad (27)$$

$$v(l,m)=\frac{g}{f}\left[\frac{h(l+1,m)-h(l-1,m)}{2\Delta x}\right] \quad (28)$$

in the Eulerian coordinates and

$$u(k)=-\frac{g}{f}\left[\frac{h(k+1)-h(k-1)}{2D}\right], \quad (29)$$

$$v(x,k)=\frac{2\pi}{x_0}B_0u(k)\cos\frac{2\pi x}{x_0} \quad (30)$$

in the quasi-Lagrangian coordinates where $g=1.4$ m sec^{-2}, $\Delta x=6\cdot10^4$m and $f=10^{-4}$ sec^{-1}. Thus, initially in the spectral model the variables h and u were completely prescribed by the mean terms in the Fourier series; y by the mean term and the first harmonic (sine term); and v by the first harmonic (cosine term). Fig. 1 shows the initial conditions for height and velocity magnitude used for the numerical solution. The initial conditions for the spectral solution were the same except for small differences near the northern and southern boundaries.

With these initial conditions, the calculations were carried out to 96 hours in the numerical model and to 92 hours in the spectral model. This limit was imposed in the latter case because by that time the spectral solution had become subject to large errors due primarily to the limited number of harmonics allowed.

8. Results of calculations

Figs. 2 and 3 show the velocity magnitude distribution after 48 and 84 hours computed by both methods. These results show a slow increase in the north-south amplitude of the isopleths of velocity magnitude with a doubling of this amplitude by 84 hours. This increase is fastest along the jet axis and slowest in the southern portion of the jet, and generally greater in the isotachs than the height contours. A small-amplitude velocity maximum which appears early in the calculation at the ridge position is observed to move eastward at a speed approximately one-half of the fluid speed in the jet axis. There is essentially no increase in velocity magnitude at the jet axis, and increases in velocity gradients are small. The height field and the isotach pattern show a correspondence throughout the calculations consistent with an approximate geostrophic relationship.

These figures show the close agreement between both methods of solution. At 48 hours (Fig. 2) there is essentially no difference between the spectral and numerical solutions. Minor discrepancies do exist near the rigid boundaries where the initial conditions were slightly different. At 84 hours (Fig. 3) the spectral

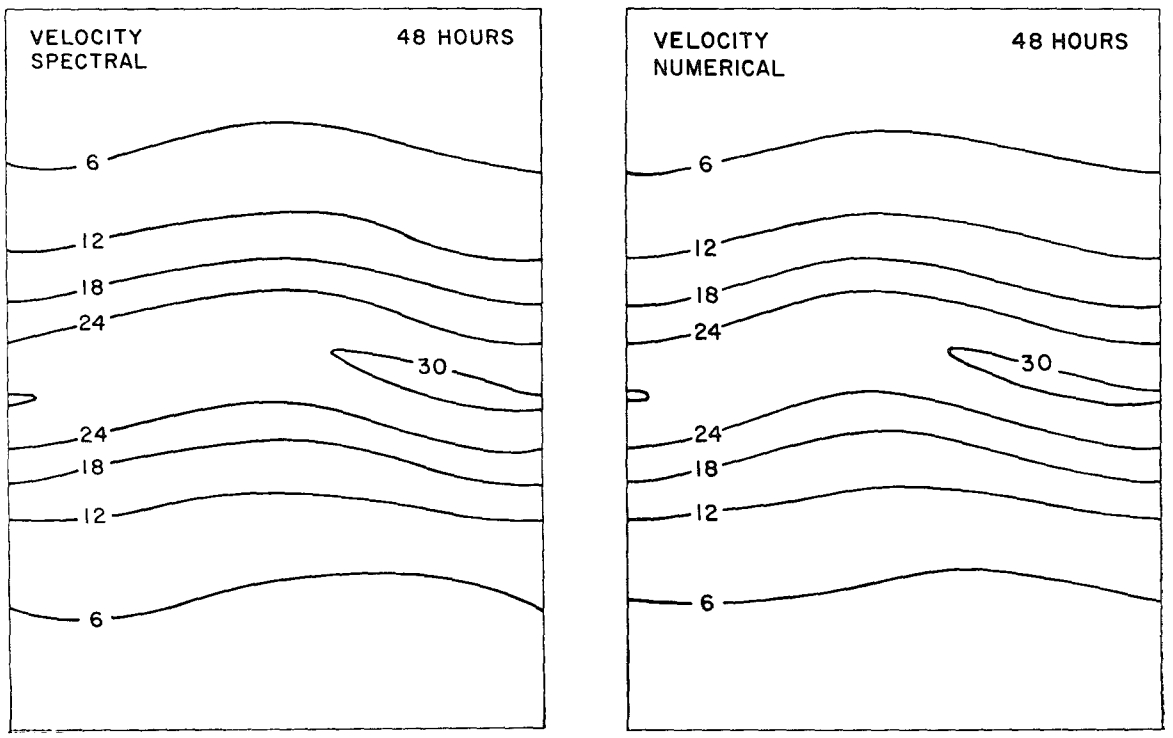

FIG. 2. Computed velocity magnitude (m sec^{-1}) after 48 hours. The spectral solution is on the left and the numerical solution on the right. Distance scale is the same as in Fig. 1.

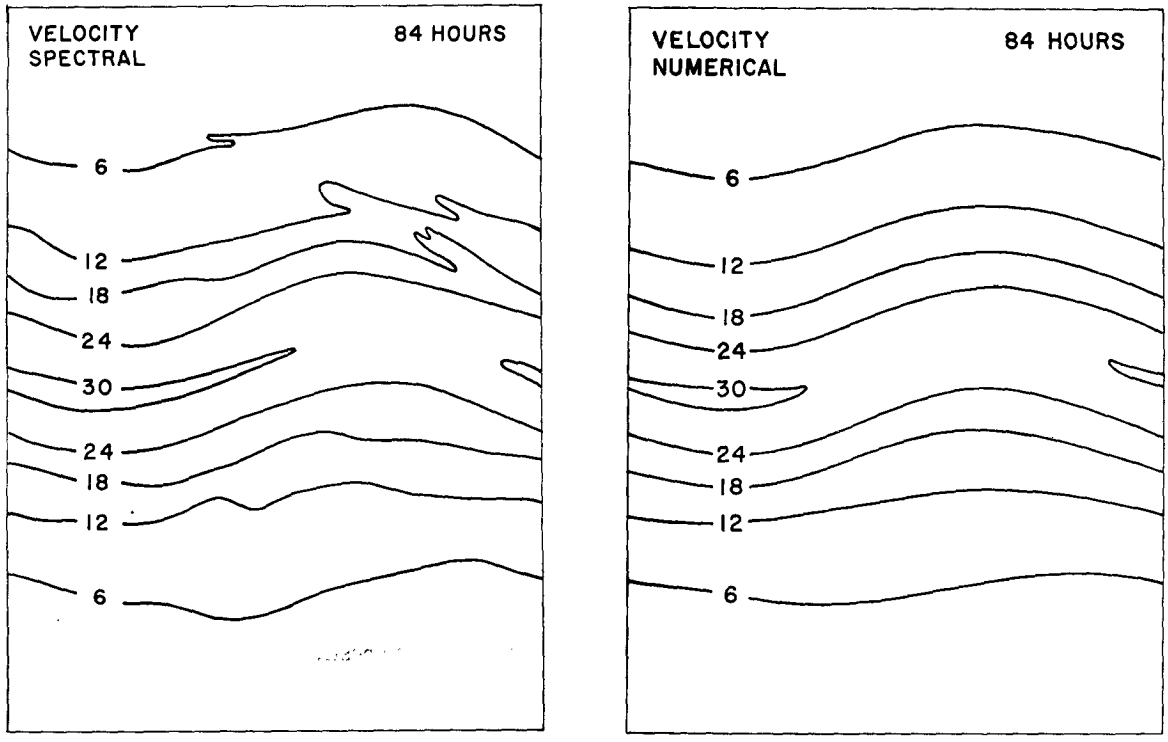

FIG. 3. Computed velocity magnitude (m sec^{-1}) after 84 hr. The spectral solution is on the left and the numerical solution on the right. Distance scale is the same as in Fig. 1.

solution has small-scale irregularities present although the patterns are still similar to those in the numerical solution. By this time the first and second harmonic magnitudes have become comparable so that the solution is subject to great truncation error.

Another comparison of the two methods with each other and with the physical model may be made with the integrated kinetic, potential and total energies. Fig. 4 shows the comparison with the values at six-hour intervals. The discontinuities present are due to the coarse print-out interval. The spectral and numerical solutions show great similarity in changes in the kinetic and potential energy up to 72 hours. The magnitude of the changes is small as a result of the approximate geostrophic condition. Differences in absolute magnitude are due to differences in the initial conditions and are not indicated according to the scales shown. Both methods give a constant total energy for the first 72 hours which is expected from the physical equations.

The comparisons demonstrate the suitability of the spectral representation together with the quasi-Lagrangian coordinates. Only two harmonics for the x-dependency of the variables provide satisfactory solutions for about 72 hours, considering the numerical solution to be the control.

An examination of the spectral components provides additional information concerning the solution. Fig. 5 shows spectral components for x-component of velocity at an instant after the initial time and at 24 and 48 hours during which time the second harmonic magnitudes are much smaller than the first. Changes in the mean values are too small to be indicated with the scales provided. Harmonics of the variables grow fastest adjacent to, but not at, the jet axis. The plots for phase angle of the maximum value of the harmonics show the effect of fluid advection near the jet axis and the differences between development on the northern and southern sides of the jet. The phase position of the first harmonic during its initial development is consistent with the tendency towards super-geostrophic velocity at the ridge position. The simplicity of the patterns shown in Fig. 5 demonstrates a clear representation of jet flow evolution that may be possible with quasi-Lagrangian coordinates.

The most interesting result observed in the quasi-Lagrangian model is the solution for the coordinate material lines. Fig. 6 shows the positions of selected material lines after 48 and 84 hours. Initially all these lines were in phase, were equidistant in the north-south direction and had a shape identical to the height isopleths in Fig. 1. The changes occurring in the distribution and shape of these lines are more drastic than the changes in the height and velocity magnitude isopleths. The small irregularities indicated at 84 hours are due to truncation errors. The effect of advection is clearly indicated by the rapid eastward movement of the patterns in the material lines in the region of the jet stream.

Much may be learned by the relationship of the ma-

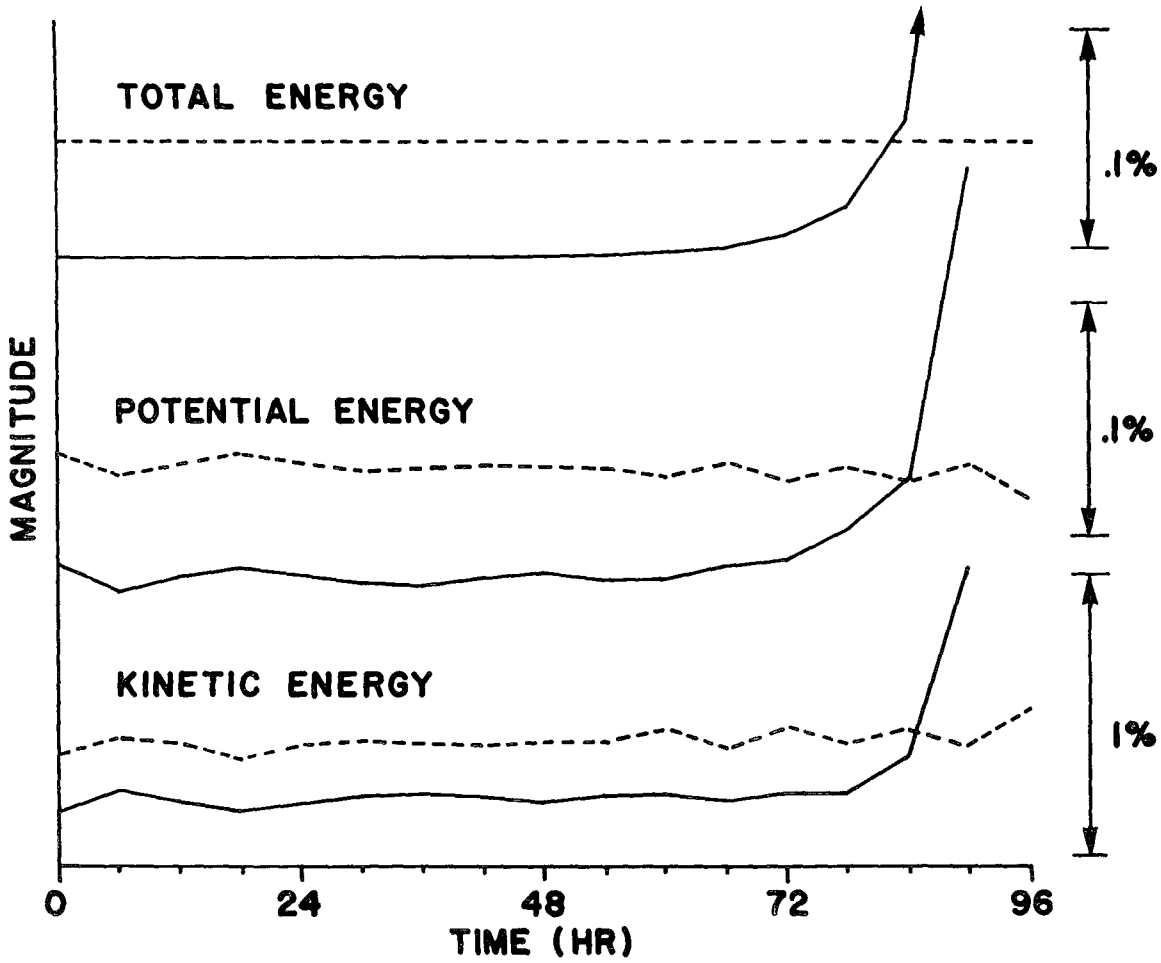

FIG. 4. Integrated energies for the spectral solution (solid line) and numerical solution (dashed line) at 6-hr intervals. All changes in absolute magnitude are shown in the same scale but each curve has a different reference for absolute magnitude. The scales at the right indicate the relative magnitude of the changes for each energy type considering potential energy to be the available potential energy and total energy to be equal to the kinetic plus the available potential energy.

terial lines to the jet flow. Fig. 7 shows the height and velocity magnitudes at 72 hours with the positions of some material lines superimposed on them. At this time the agreement between the spectral and numerical solutions is still very good which strongly implies the correctness of the positions of the material lines. Near the center of the jet the material lines are still lined up with the jet axis. Along the sides of the jet, the material lines intersect the isopleths and contours of height quite noticeably.

If the flow had been non-divergent, no intersections would have developed between the material lines and the height contours. This may be shown by making the assumption of non-divergence in Eq. (7). Then this equation simplifies to

$$\frac{\partial h}{\partial t}+u\frac{\partial h}{\partial x}+v\frac{\partial h}{\partial y}=0$$

or

$$\frac{dh}{dt}=0, \tag{31}$$

where d/dt represents the substantial derivative or the derivative following a fluid particle. Eq. (31) indicates that the height, h, would remain constant following a fluid particle making h a conservative quantity for the flow. Since h is initially constant along each coordinate material line and since each of these material lines consists of the same fluid particles for all time by definition, h would always be constant along each of these material lines. Thus the contours of height would have remained coincident with these material lines for non-divergent flow.

The development of the intersections indicates two processes in the fluid. The first is divergent motion shown by the development of gradients in height along the material lines where initially there was none. The movement and deformation of the lines suggest that the

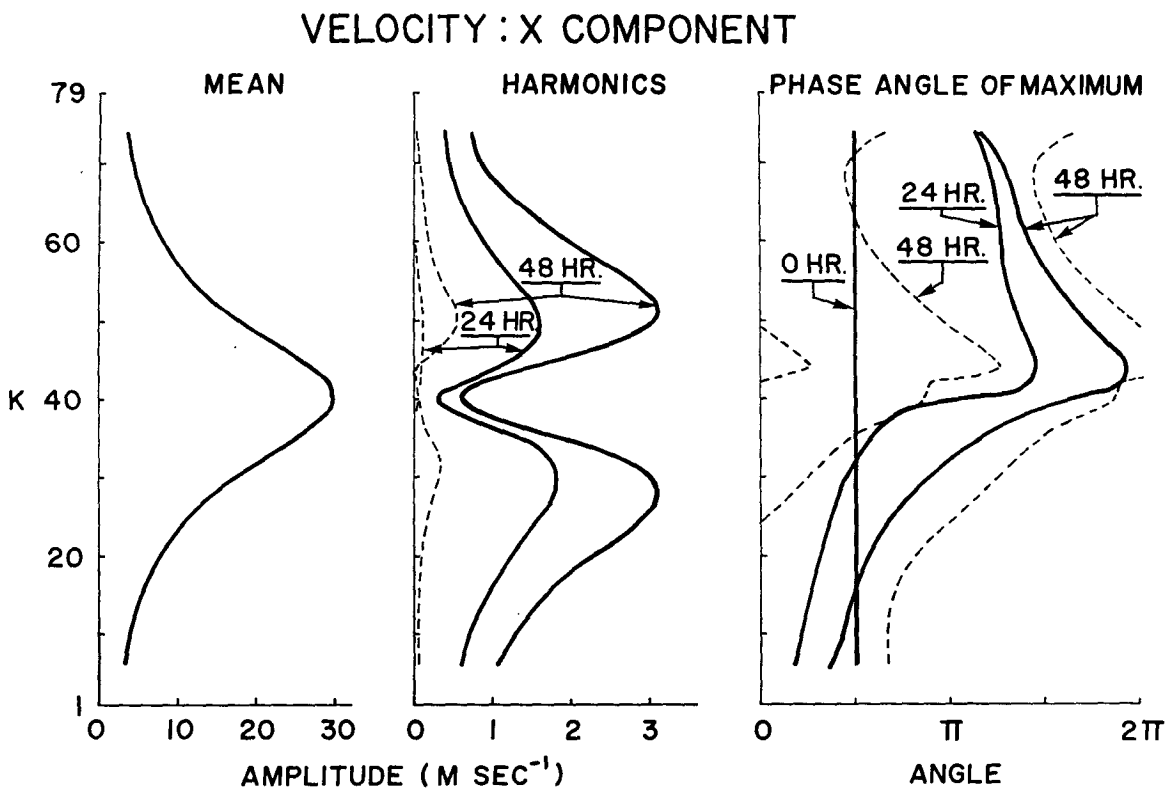

FIG. 5. Spectral components for the x-component of velocity. Solid lines indicate the first harmonic and dashed lines the second harmonic in the two graphs on the right. The phase angles for the maximum of the second harmonic are shown only for 48 hours. The ordinate is the Lagrangian variable, k.

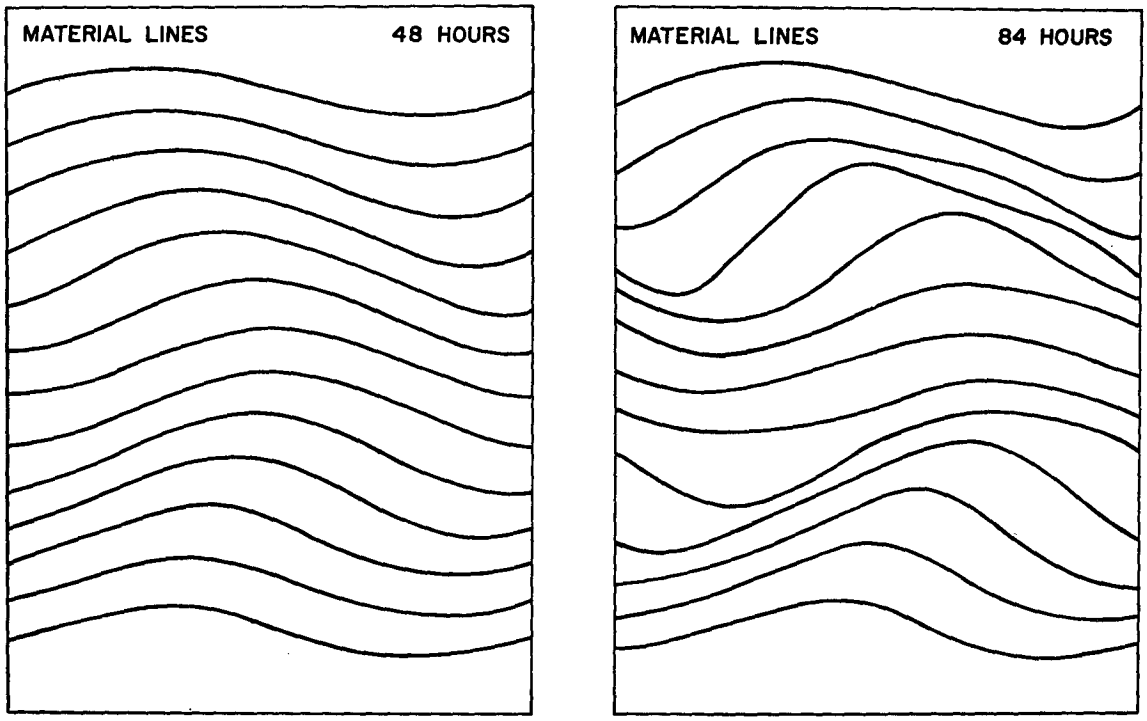

FIG. 6. Positions of selected material lines of the quasi-Lagrangian coordinate system from the spectral solution. Distance scale is the same as in Fig. 1.

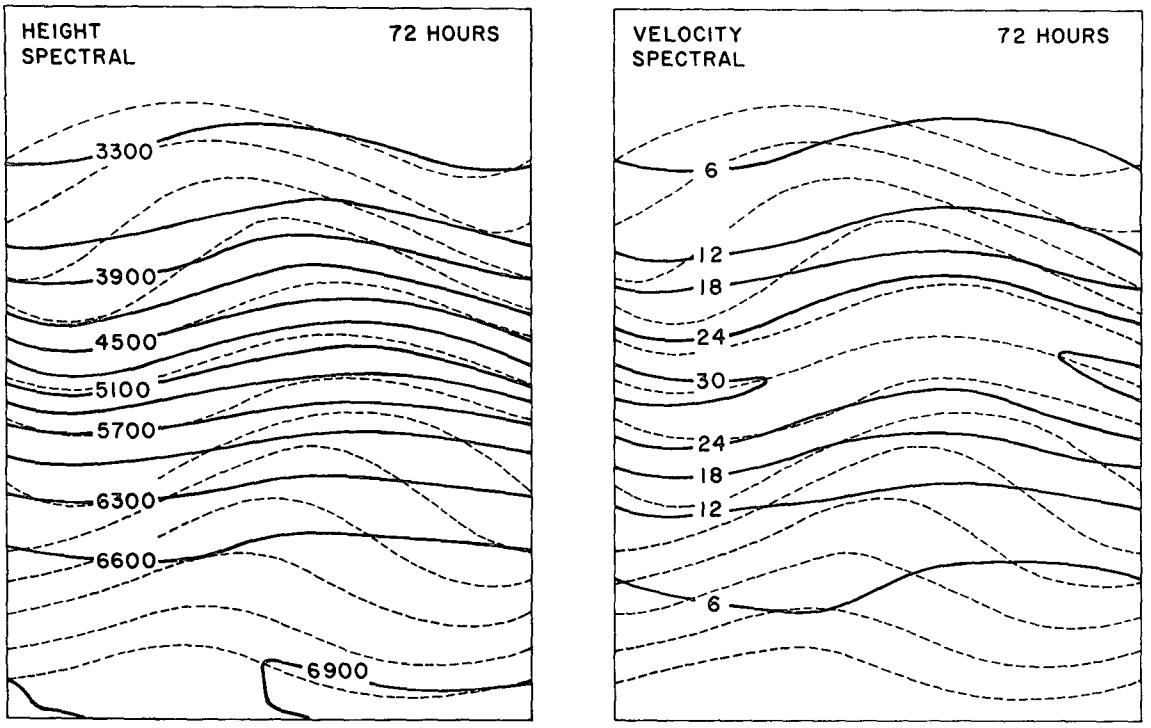

FIG. 7. Height (m) and velocity magnitude (m sec^{-1}), shown in solid lines, and selected material lines of the quasi-Lagrangian coordinate system, shown in dashed lines, from the spectral solution. Distance scale is the same as in Fig. 1.

divergent motion field corresponds to a gravity-inertial wave motion continually forced by the advective motions. The increase in north-south amplitude of material lines near the jet axis in excess of that occurring at the jet axis suggests the wave motion, and the north-south variation in the rate of eastward progression of the material line patterns suggests the forcing. Such an interpretation implies the presence of non-linear adjustment motions. The second process is indicated in Fig. 7 by the fact that the material lines consist of fluid particles. The change in position of these lines with respect to the jet flow indicates that some fluid particles have moved from less to more intense regions of the jet and vice versa. This demonstrates a mixing associated with the motions which would not be disclosed without the use of fluid particle tracers.

9. Conclusions and remarks

The results of this study show that quasi-Lagrangian coordinates are useful in the analysis of a particular ageostrophic flow problem. Indeed, successfully representing non-linear motion in part by only two harmonics suggests that analytical solutions may be possible with the coordinate system. The spectral solution is valid long enough to show the evolution of the jet flow and the non-linear processes occurring.

Nevertheless, questions may be raised as to how generally quasi-Lagrangian coordinates can be used. The limitations of the spectral method may be avoided either by using many more harmonics or by resorting to a complete finite-difference method. The problem of deformation of the material lines in the two-dimensional problem can be handled by redefinition of the lines or by choosing a problem where excessive deformation will not occur. However, in baroclinic models there will be the additional problem that the material elements will be surfaces that in general slope with height making computation of pressure even with the hydrostatic assumption tedious. It may be said that the quasi-Lagrangian system used here has many drawbacks for general prediction calculations, but in theoretical research these can be avoided by using the appropriate specialized models to demonstrate more general principles.

Physically, the Lagrangian viewpoint may be essential to understanding certain atmospheric phenomena. Riehl and Fultz (1957) showed that analyzing a jet stream flow relative to its axis could give results quite different from an Eulerian approach. Synoptic studies by Danielsen (1959) have indicated the presence of synoptic-scale mixing associated with baroclinic jet flows. Such processes as these might be more clearly understood with a Lagrangian approach.

Acknowledgments. I wish to thank Profs. George W. Platzman, The University of Chicago, and Edward N. Lorenz, Massachusetts Institute of Technology, for

their encouragement and advice in the formative stages of this study. In addition, I wish to express gratitude to Drs. Deardorff, Kasahara, and Washington, National Center for Atmospheric Research, and my wife, Barbara, for their comments and suggestions in the preparation of the manuscript. The numerical computations were carried out by Mr. Jack Miller and Mr. Larry Williams.

REFERENCES

Danielsen, E, 1959: The laminar structure of the atmosphere and its relation to the concept of a tropopause. *Archiv Meteor. Geophys. Bioklim*, Ser. A., **11**, 293–332.

Eliassen, A., 1949: The quasi-static equations of motion with pressure as independent variable. *Geofysiske Publikasjoner*, **17**, No. 3, Oslo, Det Norske Videnskaps-Akademi, 44 pp.

——, 1962: On the use of a material layer model of the atmosphere in numerical prediction. *Proc. Internat. Symposium on Numerical Weather Prediction*, Tokyo, Meteor. Soc. of Japan, pp. 207–211.

Freeman, J. C., and Staff Members, 1956: Barotropic models of the planetary jet stream. Scientific Report No. 12—Contract AF 19(604)-559, Dept. of Oceanography and Meteorology, Texas A. and M. College, College Station, Texas, 98 pp. (ASTIA No. AD98782).

Hildebrand, F. B., 1956: *Introduction to Numerical Analysis*. New York, McGraw-Hill Book Company, Inc., 511 pp.

Hinkelmann, K., 1951: Der mechanismus des meteorologischen lärmes. *Tellus*, **3**, 285–296.

Phillips, N. A., 1960: On the problem of initial data for the primitive equations. *Tellus*, **12**, 121–126.

Richtmyer, R. D., 1963: A survey of finite difference methods of non-steady fluid dynamics. NCAR Tech. Note 63-2, National Center for Atmospheric Research, Boulder, Colo. 25 pp.

Riehl, H., and D. Fultz, 1957: Jet stream and long waves in a steady rotating-dishpan experiment: structure of the circulation. *Quart. J. R. Meteor. Soc.*, **83**, 215–231.

Starr, V. P., 1945: A quasi-Lagrangian system of hydrodynamical equations. *J. Meteor.*, **2**, 227–237.

Thompson, P. D., 1957: A heuristic theory of large-scale turbulence and long-period velocity variations in barotropic flow. *Tellus*, **9**, 69–91.